

Optimization of a 3D UHF cubic antenna with quasi-isotropic radiation pattern for RFID, WSN and RSN applications

Abdelhamid BOU-EL-HARMEL ⁽¹⁾, Ali BENBASSOU ⁽²⁾, Jamal BELKADID ⁽³⁾

Laboratory of Transmission and Processing Information Eq. EMC / Telecom

Sidi Mohamed Ben Abdellah University, High School of technology

Road IMOUZZER, BP 2427, Fez

Morocco

⁽¹⁾ Abdelhamid.bouelharmel@usmba.ac.ma, ⁽²⁾ ali.benbassou@usmba.ac.ma, ⁽³⁾ belkadi@gmail.com

Abstract: - In this article, the conceptions of miniaturization of a 3D cubic antenna are presented and discussed. The miniature 3D cubic antenna is designed to operate in the UHF band [902-928 MHz] (centered at 915MHz), produce a quasi-isotropic radiation pattern and have a miniaturized size which gives us a low cost, light weight and a compact size device for RFID, WSN and RSN applications. The size of this antenna was reduced from 30 x 30 x 30 mm³ to 13.48 x 13.48 x 13.48 mm³ that implies a reduction in volume of 90.9279% and a reduction in electrical size of 54.35%. A T-match configuration has been added in order to adapt the input impedance of the antenna to the 50 Ω value. The circuit and radiation parameters simulated by HFSS and CST of the miniaturized antenna show good agreement. The form of the antenna allows to easily envelope the circuits of sensors in its interior, to reconfigure it for many values of impedances, and to operate it in other ISM bands by adjusting their geometric parameters.

Key-Words: - 3D cubic antenna; Radio Frequency Identification (RFID); Wireless sensor network (WSN); RFID sensor network (RSN); Quasi-isotropic radiation; Dipole antenna; T-match; Liquid crystal polymer LCP.

1 Introduction

The RFID sensor network (RSN) is an important wireless networking technology belongs to the Wireless Personal Area Network (WPAN). It forms a new research area that has sought the interest of both the industrial and research community. This new technology is the result of the integration of the radio frequency identification (RFID) technology [1] and wireless sensor network (WSN) technology [2] because there are a number of advantages by merging of the two technologies to satisfy the needs of specific applications [3-6].

The RSN architectures are possible architectures of integrated RFID and WSN, based on the research [3-6], there are four types of integrations class and in each scenario integration of the RSN is composed of various devices:

- Integration of RFID tags with sensors.
- Integration of RFID tags with sensors WSN nodes.
- Integration of RFID readers with WSN sensor nodes.
- Mix of RFID and WSN.

In the applications RSN, antennas play an important role in the wireless communication between the nodes of this network. There are many types of antennas operating at UHF frequencies

located below the GHz such as the planar antennas and the three-dimensional (3D) antennas. For planar antennas [7] [8], they always determine the size of the RSN node and for 3D antennas [9-12], they allow the housing of the electronic sensor in its interior so they hold the majority of the overall volume of the RSN node. Therefore, a significant reduction in size compared to planar antennas.

Miniaturization of planar or 3D antennas for the RSN is one of the most important challenges. It can play several essential roles and bring great interest for several reasons: Reduce the cost and weight of the nodes involving less material and make them more discreet and more compact i.e. allows it to take small space.

Our goal in this work will focus on the contribution to the development of these technologies based on the miniaturization of a 3D cubic antenna that we have already designed in a preceding work [12].

In the preceding work, we designed a 3D cubic antenna consisting of a single dipole having an inductively coupled supply and wound into a cubic of dimensions 27.8 x 27.8 x 20.78 mm³. This antenna operates in a higher frequency band to the desired band UHF [902-928 MHz] (centered at 915

MHz), then we have increased its size to 30 x 30 x 30 mm³ [12].

In the present work, we will make a parametric study of the previous antenna [12] for that the antenna be miniaturized on condition that it will work in the UHF frequency band [902-928 MHz] (centered at 915MHz) and that it produces a quasi-isotropic radiation. In the first step, we will keep the cube size to 27.8mm and varying the structure of the dipole to attain the condition. Then we will continue the variation with decreasing the size of the antenna until its miniaturization. Then, we will mix the above structures until the condition is achieved. There are some parts of the dipole which are not rolled in the same direction of current so we will reduce these parts with decreasing the antenna size order to improve the radiation pattern. Finally, we will eliminate all these parts and we will find a miniature 3D cubic antenna with good radiation characteristics.

Note that the design and simulation were carried out using the 3D electromagnetic simulator, HFSS (High Frequency Structure Simulator) that is based on the finite element method (FEM). The use of this simulator has helped us to study the geometric parameters of the antenna to determine the effect of each parameter and to determine an optimal value for each. The final results of simulation were compared by the CST Microwave Studio simulator (Computer Systems Technology) which is based on the finite integration technique (FIT).

2 Miniaturization of the 3D cubic antenna

The first antenna designed in the preceding work [12] is presented in Fig. 1 (b), this antenna is the result of folding of the structure of Fig.1 (a) in cubic form. The substrate used as support is the liquid crystal polymer (LCP) of relative permittivity $\epsilon_r = 3$ and dielectric loss tangent $\tan \delta = 0.002$ due to their mechanical flexibility and excellent electrical performance [13].

To attain on the condition that we have, it must be varied the dipole structure without varying the overall size of the antenna. According to Fig. 1, it exists two junction angles α_1 and α_2 . The first angle α_1 is between D2 and D3, and the second angle α_2 between D4 and D5. We proposed a reduction of the junction angles, which involves the increase in the length of the dipole.

First of all, we reduced the angle α_1 on the one hand by the increasing rectilinear of the length D2 and on the other hand by the increasing rectilinear

of the length D3 as present in Fig. 2 (a) (b). Then, we reduced the angle α_2 , on the one hand by the increasing rectilinear of the length D4 and secondly by the increasing rectilinear of the length D5 as shows in Fig. 2 (c) (d). A T-match configuration was added to each antenna to adapt the input impedance to 50 Ω (Fig.2 (e)).

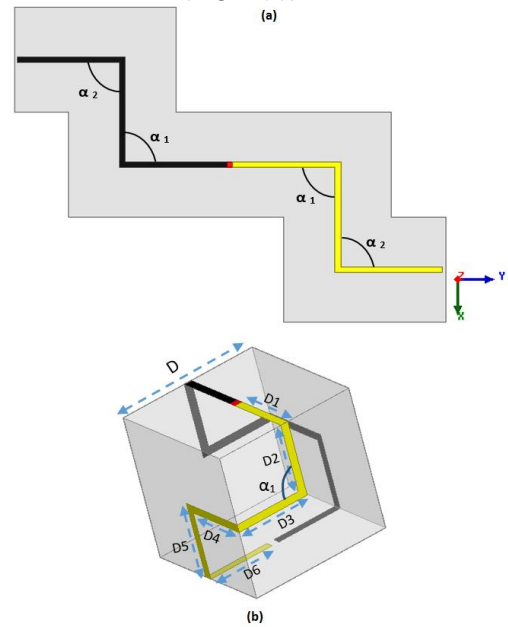


Fig. 1. Structure of the 3D cube antenna : (a) before folding, (b) after folding.

TABLE I. Dimensions of the 3D cubic antenna.

Parameters	D, D1	D2, D4, D6	D3, D5	α_1, α_2
Values	27.8mm	13.15mm	14.65mm	90°

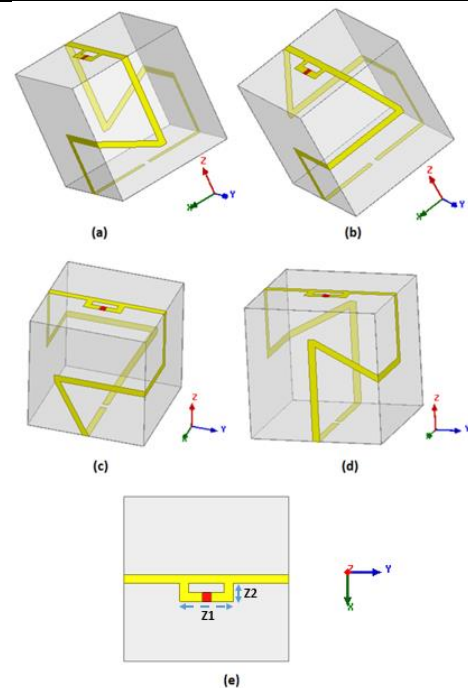


Fig. 2. Structures of 3D cubic antenna (D = 27.8) : (a) Increase in D2, (b) Increase in D3, (c) Increase in D4, (d) Increase in D5, (e) T-match configuration.

The return loss S_{11} simulated by HFSS of each antenna structure of Fig.2 is shown in Fig.3. The dimensions of the T-match configuration and the junction angles of each antenna with the results of the simulation are listed in Table II.

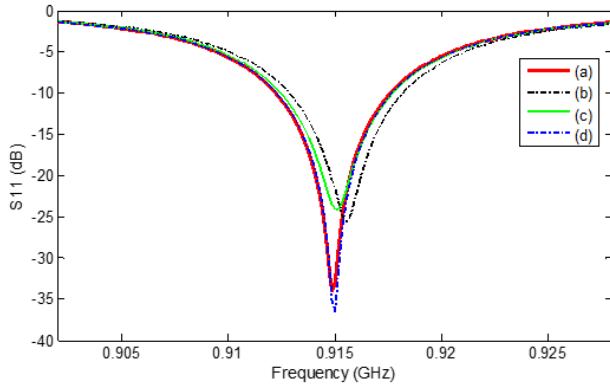


Fig. 3. Return loss S_{11} of each 3D cubic antenna structure (Fig.2).

TABLE II. The dimensions of T-match and of the junction angles of each antenna with the results of the simulation.

Structures	(a)	(b)	(c)	(d)
α_1 (°)	61.94	64.05	90	90
α_2 (°)	90	90	61.63	59.1
Z1 (mm)	9	9	9	9
Z2 (mm)	3	3	3	3
S_{11} (dB)	-33.98	-25.6	-24.11	-36.49
Fr (MHz)	914.9	915.5	915.1	915

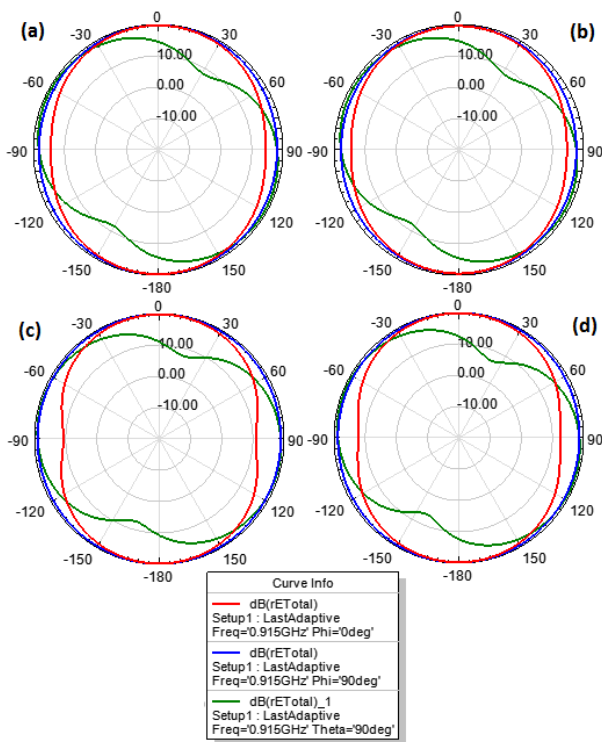


Fig. 4. Radiation patterns (E_{Total}) in 2D of each 3D cubic antenna structure (Fig.2) in the plans: xz, yz and xy.

From these results, each antenna resonates at a frequency, which is close to the desired frequency that is 915 MHz in the order with a bandwidth of 0.6% at -10 dB of S_{11} .

Concerning the radiation pattern, Fig.4 shows the radiation patterns of the total radiated electric field (E_{Total}) in dB for each antenna at 915MHz frequency in the three planes xz ($\Phi = 0^\circ$), yz ($\Phi = 90^\circ$) and xy ($\theta = 90^\circ$). From these diagrams, the variation of E_{Total} does not reach zero in all three planes and we see it well in Fig.5 that represents the radiation patterns in all 3D space, so the diagrams are yet quasi-isotropic. Therefore, we achieved our previous goal.

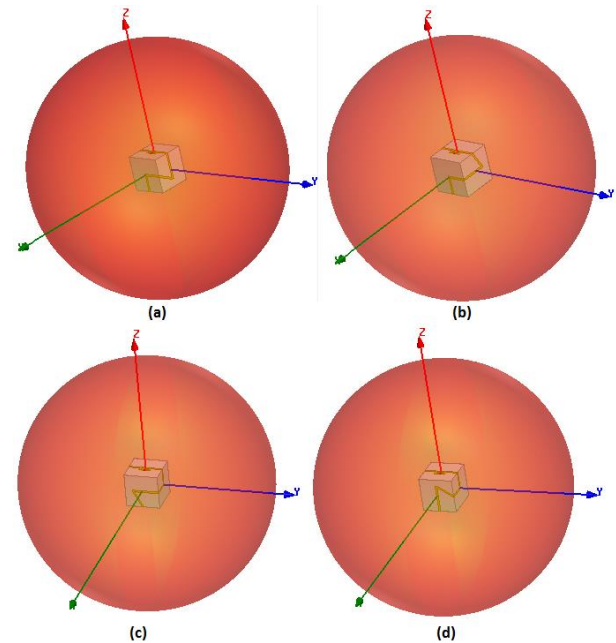


Fig. 5. Radiation patterns (E_{Total}) in 3D of each 3D cubic antenna structure (Fig.2).

Now, we can reduce the antenna size and continue the decrease in junction angles α_1 and α_2 at the same time until the distance between the radiating element and the edge of the cubic substrate is equal to 0.5mm. Fig.6 shows the different four new 3D cube antenna structures.

Fig.7 shows the variation of the return loss S_{11} simulated by HFSS depending on the frequency of each antenna structure of Fig.6. The dimensions of the T-match, the values of the junction angles and the size of each antenna with the results of the S_{11} simulation are listed in Table III.

According to the results, all antennas resonate at a frequency that is close to the desired frequency with a bandwidth varies depending to the size of each antenna (0.423% (a), 0.238% (b) 0.345% (c) and 0.325% (d) at -10 dB of S_{11}).

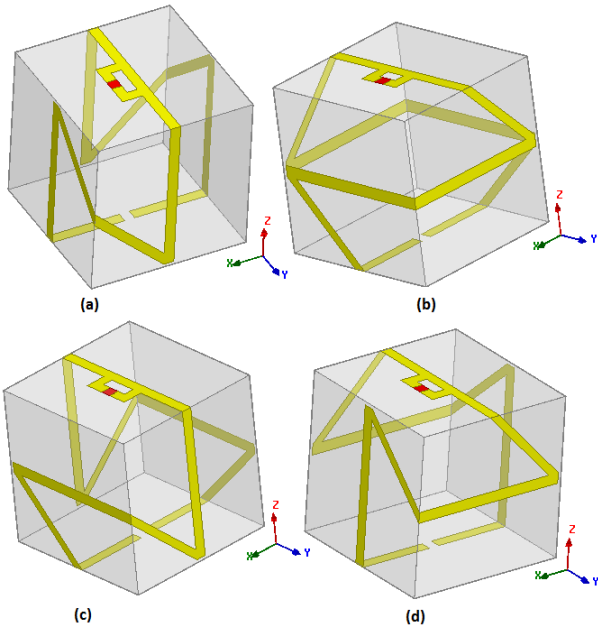


Fig. 6. Structures of 3D cubic antenna : (a) Increase in D2 and D5, (b) Increase in D3 and D4, (c) Increase in D2 and D4, (d) Increase in D3 and D5.

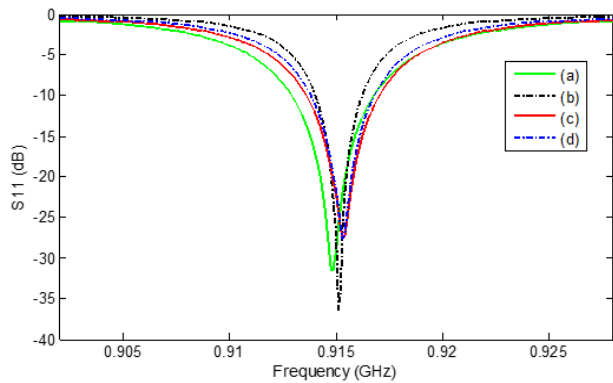


Fig. 7. Return loss S_{11} of each 3D cubic antenna structure (Fig.5).

TABLE III. Dimensions of the T-match, the junction angles and the size of each antenna with the simulation results.

Structure	(a)	(b)	(c)	(d)
D (mm)	22.97	21.44	22.78	22.54
α_1 (°)	46.366	46.473	46.378	46.394
α_2 (°)	46.366	46.473	46.378	46.394
Z1 (mm)	7.5	5.5	7	6.5
Z2 (mm)	3	3	3	3
S_{11} (dB)	-31.48	-36.4	-27.57	-27.6
Fr (MHz)	914.9	915.1	915.3	91

The Fig.8 presents the radiation patterns of E Total field radiated in dB for each antenna of the Fig.6 at 915MHz frequency in the three planes xz ($\theta = 0^\circ$), yz ($\theta = 90^\circ$) and xy ($\theta = 90^\circ$).

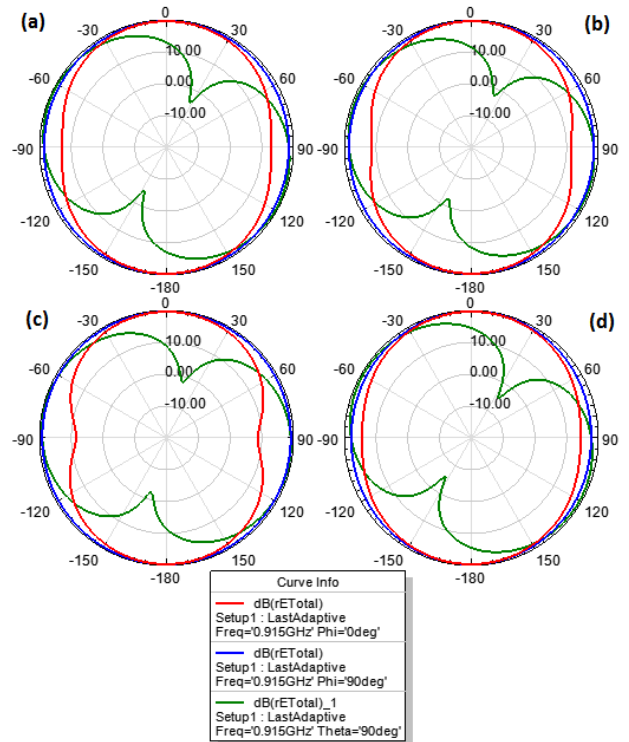


Fig. 8. Radiation patterns (E Total) in 2D of each 3D cubic antenna structure (Fig.6) in the plans: xz, yz and xy.

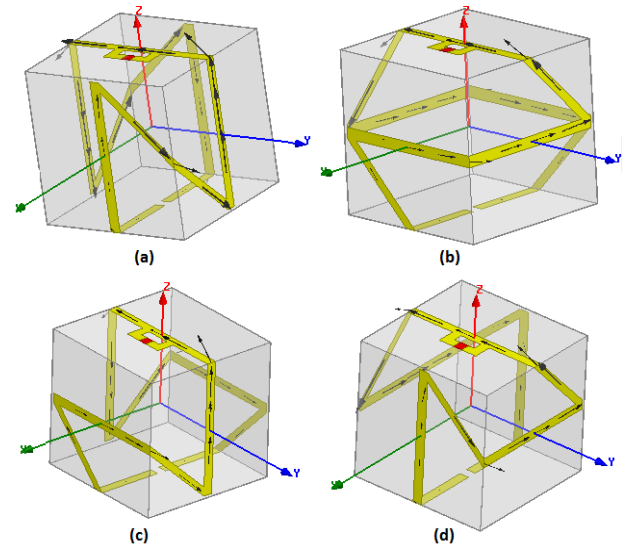


Fig. 9. Current directions in the two arms of each antenna (Fig.6).

From these diagrams, the E Total variation of each 3D cubic antenna in the xz and yz planes does not reach zero but in the xy plane we see that the E Total exceeds zero towards negative values, which implies that all these antennas does not produce a quasi-isotropic radiation pattern. That is because there are a large parts in the two arms of the dipole are not wound in the same current direction as shown in Fig. 4 (for the antenna (a): D3 and D4, (b): D2 and D5, (c): D3 and D5, and (d): D2 and D4). Whereas we have not achieved our goal.

After the 3D cubic antenna structures of fig.6, we posed a question “Does the mixture of these structures can lead us to reach the condition?” Therefore, we designed this antenna as shown in Fig. 10 to respond to this question. We illustrated his dimensions in Table IV.

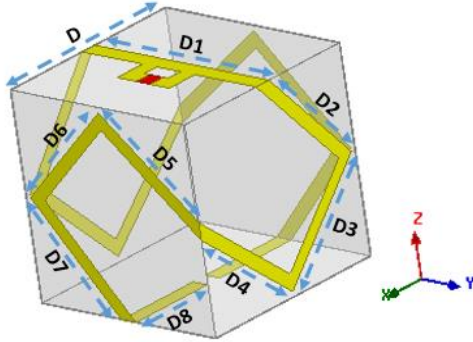


Fig. 10. Structure of the 3D cubic antenna which is the result of mixing.

TABLE IV. The dimensions of the antenna (Fig.10) with the T-match configuration.

Parameters	D, D1	D2, D4, D5, D7	D3, D6	D8	Z1	Z2
Values (mm)	18.36	12.13	12.28	8.43	5.5	3

Fig.11 shows the variation of return loss S_{11} simulated by HFSS according to the frequency of the antenna Fig.10. A minimum value of S_{11} is -20.77 dB at the resonance frequency of 915.4 MHz, which is close to the desired frequency of the order of 915 MHz with a bandwidth equal to 0.21%.

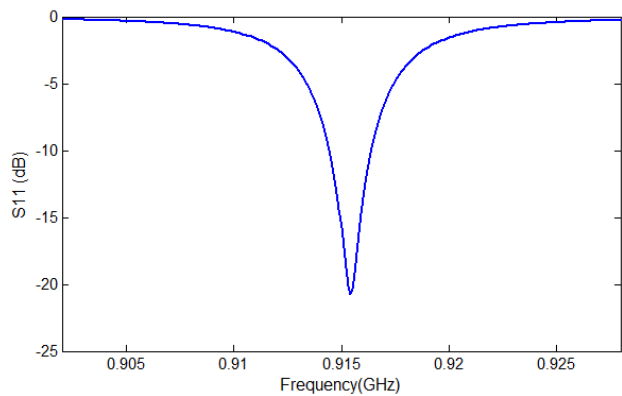


Fig. 11. Return loss S_{11} of the antenna (Fig.10).

The radiation pattern of the total field radiated in dB at 915MHz frequency of antenna of the Fig.10 in the three planes xz ($\phi = 0^\circ$), yz ($\phi = 90^\circ$) and xy ($\theta = 90^\circ$) is shown in Fig.12.

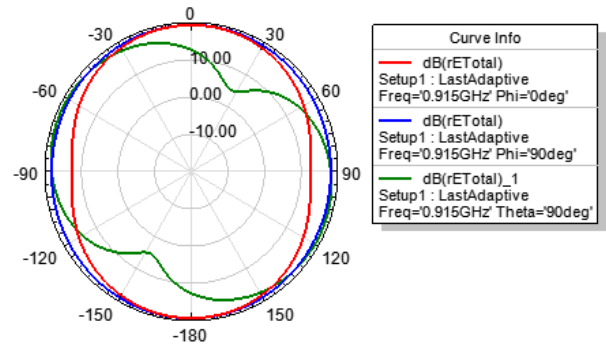


Fig. 12. Radiation pattern (E Total) in 2D of the antenna (Fig.10) in the plans: xz, yz and xy.

From the diagram, the variation of the E Total in the xz and yz planes does not reach zero as before. In the xy plane, variation E Total has a minimum value equal to 4.3675dB, which is greater than zero. According to Fig.13, which shows the radiation pattern in 3D, the antenna produces a quasi-isotropic radiation pattern.

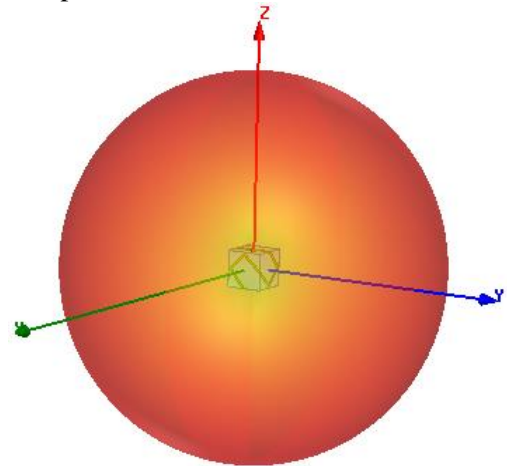


Fig. 13. Radiation patterns (E Total) in 3D of the 3D cubic antenna (Fig.10).

From the Fig.10, there are still parts in the two arms of the dipole that are not wrapped in the same current direction (D2 and D7). Therefore, we will reduce these parts by increasing the size of “f” (Fig.14 (d)) to improve the radiation pattern and minimize the size of the antenna. We designed several antennas of “f” ranges from 1.5mm to 8mm as shown in Fig.14 to notice and visualize the improvement of the radiation pattern and decreasing the size of the antenna.

The variation of the return loss S_{11} simulated by HFSS depending on the frequency of each antenna structure of the Fig.14 is shown in Fig.15. The dimensions of each antenna with T-match and the results of the simulation of S_{11} are shown in Table V.

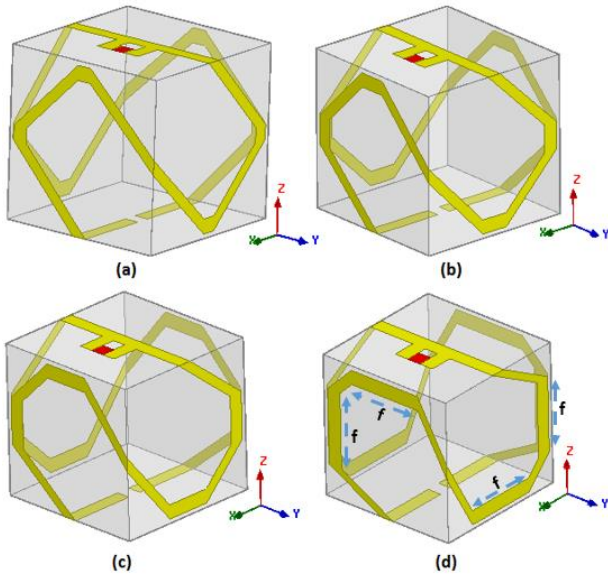


Fig. 14. Structures of the 3D cubic antenna: (a) $f = 1.5m$, (b) $f = 3mm$, (c) $f = 5mm$, (d) $f = 8mm$.

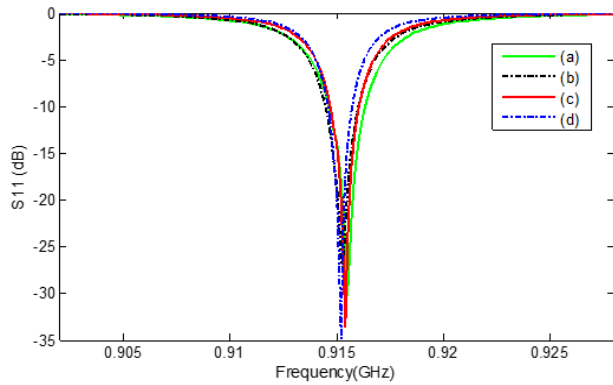


Fig. 15. Return loss S_{11} of the antenna in Fig.14.

TABLE V. Dimensions of each antenna of the Fig.14 with the T-match configuration.

Structures	(a)	(b)	(c)	(d)
D, D1 (mm)	17.58	16.92	16.09	14.88
D2, D4, D5, D7 (mm)	11.02	10.02	8.77	7.08
D3, D6 (mm)	10.66	9.136	7.135	4.16
f (mm)	1.5	3	5	8
Z1 (mm)	5	4.8	4.5	4.5
Z2 (mm)	3	3	3	2.5
S_{11} (dB)	-30.12	-27.13	-33.65	-34.85
Fr (MHz)	915.5	915.3	915.4	915.2

From the results, all antennas resonate at a frequency that is close to the required frequency with a bandwidth varies depending on the size of each antenna (0.181% (a), 0.164% (b) 0.144% (c) and 0.121% (d) at -10 dB S_{11}).

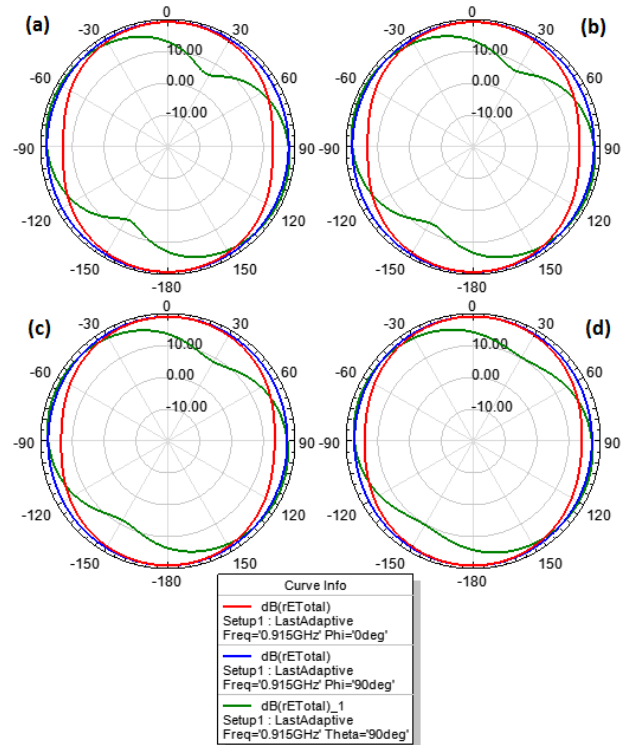


Fig. 16. Radiation patterns (E Total) in 2D of the antenna (Fig.14) in the plans: xz, yz and xy.

According to the radiation patterns shown in Fig.12 and Fig.16, The field E Total radiated variation in the xy increases of the value 4.3675dB to 10.306dB by increasing the length f of 0mm to 8mm. We made a simulation of the radiation pattern in the whole space (Fig.17) to check that the radiation patterns are quasi-isotropic.

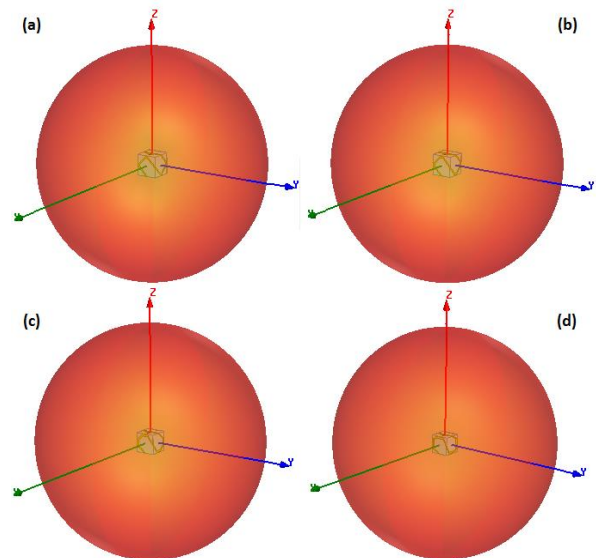


Fig. 17. Radiation patterns (E Total) in 3D of antennas of the Fig.14.

Therefore, in this part we have improved the radiation pattern of the 3D cubic antenna with minimizing its size with success (Table V).

We can continue increasing “f” but when “f” tends to the size of the antenna, the width D2, D4, D5 and D6 tends towards zero. Now, we will correct widths D2, D4, D5, and D6 to be equal to 1.5mm (i.e. the width of the dipole). The antenna designed in Fig.18 (b). This antenna is easily manufactured by folding the structure shown in Fig.18 (a).

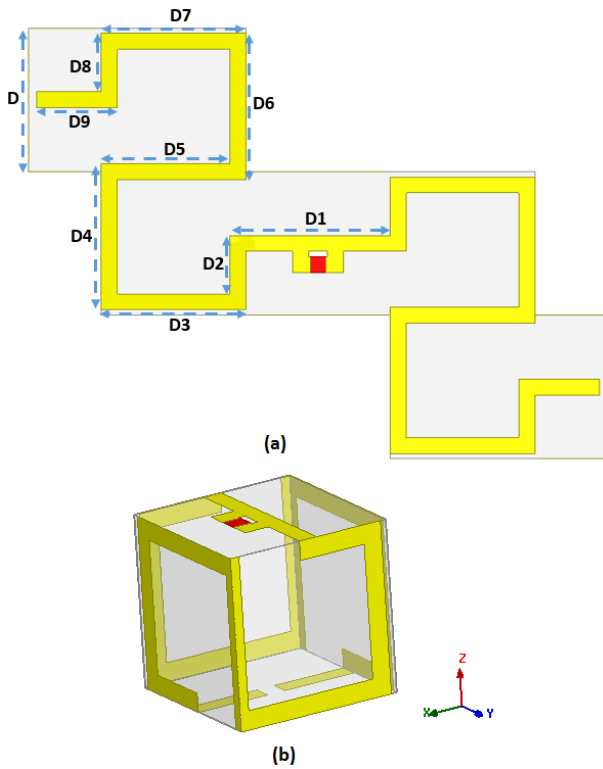


Fig. 18. Structure of the 3D cubic antenna: (a) before folding and (b) after folding.

The dimensions of the antenna adapted to the 50 Ω by T-match configuration are shown in Table VI.

TABLE VI. Dimensions of the antenna (Fig.16) with the T-match configuration.

Parameters	D, D3, D7	D1	D2, D8	D4, D6	D5	D9	Z1	Z2
Values (mm)	13.48	14.98	5.49	12.98	11.98	7.49	4.8	2.1

The circuit parameters of this antenna such as the return loss S_{11} and the input impedance Z_a simulated by HFSS and compared by CST are presented in Fig. 19.

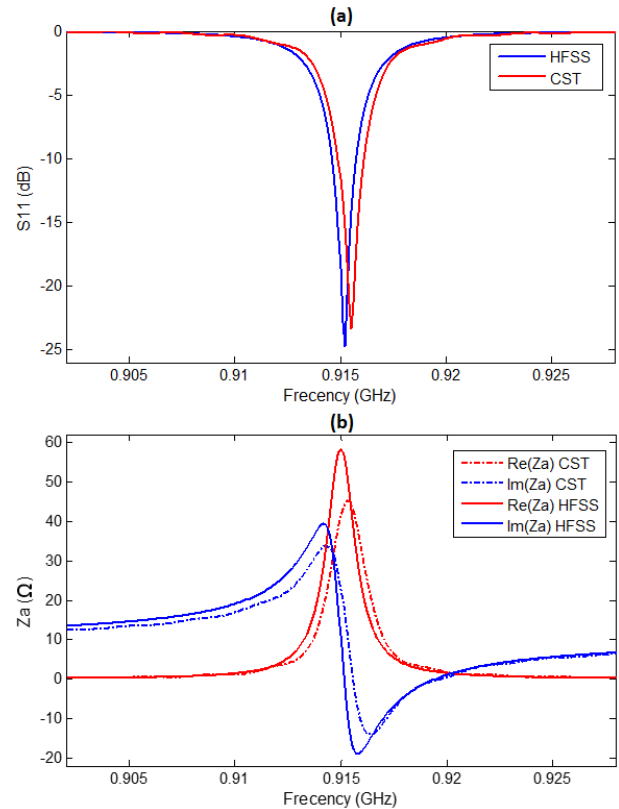


Fig. 19. Circuit parameters of the 3D cubic antenna (Fig.16) adapted to 50 Ω: (a) Return loss S_{11} , (b) Input impedance Z_a .

Based on the results of HFSS, the S_{11} of this antenna depending on the frequency reaches the level of -24.70 dB for a resonant frequency equal to 915.2 MHz, where $Z_a = 53.31 - j 2.94 \Omega$ at the same frequency with a bandwidth of the order of 0.121 %.

A minimum value of S_{11} is obtained by CST of -23.38 dB at the resonance frequency of 915.5 MHz, when $Z_a = 44 + j 2.12 \Omega$ at the same frequency with the bandwidth of the order of 0.131%.

We observe a slight difference between the results obtained by HFSS simulator and those by CST in terms of the resonant frequency, level S_{11} , Z_a value and bandwidth. This difference is due to the difference between the numerical method of each simulator with the simulation step and the mesh used during the simulation.

Radiation parameters of this antenna are simulated at the frequency 915 MHz. Fig. 20 shows the radiation pattern in 2D of the radiated E Total in dB of the antenna simulated by HFSS in xz (a), YZ (b) and xy (c) (i.e. $\phi = 0^\circ$, $\theta = 90^\circ$, $\phi = 90^\circ$ respectively).

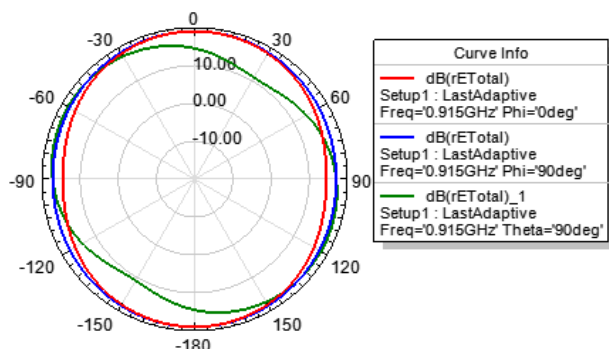


Fig. 20. Radiation patterns of the E Total in 2D of the cubic antenna in the xz, yz and xy planes.

Based on the radiation pattern, we remark that the radiated field E Total do not reached zero in all three planes. The field radiated E Total has a minimum value equal to 10.87 dB in the xy plane. Therefore, we can say that the radiation pattern is a quasi-isotropic diagram. To check that the diagram is quasi-isotropic, we made a simulation of the diagram in the whole space as shown in Fig.21.

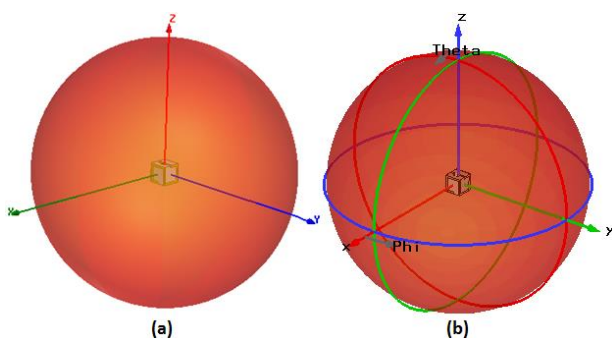


Fig. 21. Diagrammes de rayonnement (E Total) en 3D de l'antenne de la Fig.18 : (a) simulé par HFSS et (b) simulé par CST.

Gain and directivity of the antenna are also simulated; the maximum gain and directivity are respectively 1.29 dB and 1.69 dB that gives an efficiency of 76.33 %.

The size of the 3D cubic miniaturized antenna is 13.48 mm × 13.48 mm × 13.48 mm, which implies a dimension depending of the wavelength equal to $\lambda/24.3$. The antenna is classified as very small antenna view its electrical size ka equal to 0.2237 which is smaller than 0.5, where “k” is the wave number in free space $2\pi / \lambda$, and “a” is the radius of an imaginary sphere circumscribing the maximum dimensions of the antenna [14].

In order to compare this work with the work of [12], Table VII summarizes the antenna size with simulation results from HFSS.

TABLE VII. Comparison between this work and previous work [12].

Antenna	Present	[12]
Size (mm ³)	13.48 x 13.48 x 13.48	30 x 30 x 30
ka	0.2237	0.49
S ₁₁ (dB)	-24.7	-31.02
fr (MHz)	915.2	918.4
Bandwidth (%)	0.121	0.756
Radiation pattern	Quasi-isotropic	Quasi-isotropic
Gain (dB)	1.29	1.847
Efficiency (%)	76.33	97.26

From the table above, the antenna size was reduced from 30 x 30 x 30 mm³ to 13.48 x 13.48 x 13.48 mm³, which implies a reduction in the volume of 90.9279% and a reduction in the electrical size of 54.35%. The antenna resonance frequency of this work is very close to the desired frequency (915MHz) compared to [12]. Levels S₁₁ dependent adaptation. A reduction of the bandwidth, gain and efficiency because they are proportional to the size of the antenna.

We minimize the size of the antenna with a quasi-isotropic radiation pattern and a resonant frequency very close to 915MHz. The form of the miniaturized antenna provides low cost, a lightweight and a compact size device for RFID, WSN and RSN applications because the form allows enveloping easily the circuits and sensors in its interior. We can configure the antenna for many input impedance values Z_a [15] and to operate in the other ISM bands by adjusting the geometric parameters.

This antenna has a very important role in the RFID technology by eliminating the problem of not reading a tag based on dipole antennas, because it is known that the radiation pattern of a dipole has zeros along its wire axis. And a very important role in the WSN and RSN technology by eliminating intermittent communication between the network devices so it allows network nodes to communicate well each with others independently of the orientation.

4 Conclusion

In this work, a 3D cubic antenna miniature form was proposed. We have done studies of geometrical parameters of the antenna to determine the effect of each parameter for miniaturization of the size of the antenna with the condition that it must operate in the UHF frequency band [902-928 MHz] and produce a quasi-isotropic radiation. The size of the 3D cubic miniaturized antenna is 13.48 mm × 13.48 mm ×

13.48 mm, which implies a dimension according to the wavelength equal to $\lambda / 24.3$. From the simulation, we obtained a return loss S_{11} of -24.7 dB at 915.2 MHz, a quasi-isotropic radiation pattern with a maximum gain of 1.29 dB and an efficiency of 76.33%. This antenna has a form makes it easy to wrap the circuits and sensors in its interior and has the advantage to be miniature with lightweight and low manufacturing cost.

References:

- [1] M. Bolic, D. Simplot-Ryl, and I. Stojmenović, Eds., *RFID systems: research trends and challenges*, Hoboken, NJ: Wiley, 2010.
- [2] Qinghua Wang and Ilango Balasingham, *Wireless Sensor Networks - An Introduction, Wireless Sensor Networks: Application-Centric Design*, Yen Kheng Tan (Ed.), ISBN: 978-953-307-321-7, InTech, 2010.
- [3] H. Liu, M. Bolic, A. Nayak, and I. Stojmenovic, Taxonomy and challenges of the integration of RFID and wireless sensor networks, *Netw. IEEE*, vol. 22, no. 6, pp. 26–35, 2008.
- [4] L. Zhang and Z. Wang, Integration of RFID into wireless sensor networks: Architectures, opportunities and challenging problems, in *Grid and Cooperative Computing Workshops, 2006. GCCW'06. Fifth International Conference on*, 2006, pp. 463–469.
- [5] B. Zhang, K. Hu, and Y. Zhu, Network architecture and energy analysis of the integration of RFID and Wireless Sensor Network, in *Control and Decision Conference (CCDC)*, 2010 Chinese, 2010, pp. 1379–1382.
- [6] A. Mitrokotsa and C. Douligeris, Integrated RFID and sensor networks: architectures and applications, *RFID Sens. Netw. Archit. Protoc. Secur. Integr.*, pp. 511–535, 2009.
- [7] A. Babar, L. Ukkonen, and L. Sydanheimo, Dual UHF RFID band miniaturized multipurpose planar antenna for compact wireless systems, in *Proc. Int. Workshop Antenna Tech. (iWAT)*, Mar. 2010, pp. 1–4.
- [8] R. H. Bhuiyan, R. Dougal, and M. Ali, A new crossed staircase dipole antenna for 915 MHz RFID application, in *Antennas and Propagation Society International Symposium*, 2008. AP-S 2008. IEEE, 2008, pp. 1–4.
- [9] I. T. Nassar and T. M. Weller, Development of Novel 3-D Cube Antennas for Compact Wireless Sensor Nodes, *IEEE Trans. Antennas Propag.*, vol. 60, no. 2, pp. 1059–1065, Feb. 2012.
- [10] I. T. Nassar and T. M. Weller, An electrically-small, 3-D cube antenna fabricated with additive manufacturing, in *Power Amplifiers for Wireless and Radio Applications (PAWR)*, 2013 IEEE Topical Conference on, 2013, pp. 91–93.
- [11] I. T. Nassar, H. Tsang, K. Church, and T. M. Weller, A high efficiency, electrically-small, 3-D machined-substrate antenna fabricated with fused deposition modeling and 3-D printing, in *Radio and Wireless Symposium (RWS)*, 2014 IEEE, 2014, pp. 67–69.
- [12] A. Bou-El-Harmel, A. Benbassou, and J. Belkaid, Design of a Three-Dimensional Antenna UHF in the Form Cubic Intended for RFID, Wireless Sensor Networks (WSNs) and RFID Sensor Networks (RSNs) Applications, *International Journal on Communications Antenna and Propagation (IRECAP)*, vol 4, no. 6, pp. 260-264, 2014.
- [13] D. Thompson, *Characterization and design of liquid crystal polymer (LCP) based multilayer RF components and packages*, Ph.D. dissertation, Dept. Elect. Comput. Eng., Georgia Inst. of Technol., Atlanta, GA, 2006.
- [14] S. R. Best, *A study of the performance properties of small antennas*, Antenna Appl. Sym, pp. 193–219, 2007.
- [15] G. Marrocco, The art of UHF RFID antenna design: impedance matching and size-reduction techniques, *Antennas Propag. Mag. IEEE*, vol. 50, no. 1, pp. 66–79, 2008.